Mon. Not. R. Astron. Soc. **000**, 000–000 (0000) Printed 2 February 2008 (MN LATEX style file v2.2)

Asymptotic Giant Branch Stars in the Phoenix Dwarf Galaxy

John Menzies[1], Michael Feast[2], Patricia Whitelock[1,2,3], Enrico Olivier[1,4], Noriyuki Matsunaga[5] and Gary Da Costa[6]

[1] *South African Astronomical Observatory, P.O.Box 9, 7935 Observatory, South Africa.*
[2] *Astronomy Department, University of Cape Town, 7701 Rondebosch, South Africa.*
[3] *National Astrophysics and Space Science Programme, Department of Mathematics and Applied Mathematics, University of Cape Town, 7701 Rondebosch, South Africa.*
[4] *Department of Physics, University of the Western Cape, Private Bag X17, 7535 Bellville, South Africa.*
[5] *Department of Astronomy, Kyoto University, Kitashirakawa Oiwake-cho, Sakyo-ku, Kyoto, Kyoto 606-8502, Japan.*
[6] *Research School of Astronomy and Astrophysics, Australian National University, Mount Stromlo Observatory, Weston Creek, ACT 2611, Australia.*

2 February 2008

ABSTRACT

JHK_s near-infrared photometry of stars in the Phoenix dwarf galaxy is presented and discussed. Combining these data with the optical photometry of Massey et al. allows a rather clean separation of field stars from Phoenix members. The discovery of a Mira variable (P = 425 days), which is almost certainly a carbon star, leads to an estimate of the distance modulus of 23.10 ± 0.18 that is consistent with other estimates and indicates the existence of a significant population of age $\sim$ 2 Gyr. The two carbon stars of Da Costa have $M_{bol} = -3.8$ and are consistent with belonging to a population of similar age; some other possible members of such a population are identified. A Da Costa non-carbon star is $\Delta K_s \sim 0.3$ mag brighter than these two carbon stars. It may be an AGB star of the dominant old population. The nature of other stars lying close to it in the $K_s, (J - K_s)$ diagram needs studying.

Key words: galaxies:dwarf - galaxies:stellar content - stars:AGB and post-AGB - stars: carbon

1 INTRODUCTION

The present investigation of the Phoenix dwarf galaxy is part of a programme to study local group galaxies using the Japanese - South African 1.4m Infrared Survey Facility (IRSF) and SIRIUS three-channel camera (Nagashima et al. 1999, Nagayama et al. 2003) at SAAO Sutherland.

Phoenix is a member of the Local Group and the most distant of the Milky Way's satellite galaxies (e.g. Grebel (1999) fig. 3). It was discovered by Schuster & West (1976) who originally suggested it might be a globular cluster; Canterna & Flower (1977) established that it was a galaxy. Though its overall properties are consistent with a classification as a dwarf spheroidal, it also contains a relatively small young component and is thus often referred to as a dIrr/dSph (e.g. Mateo 1998). It is associated with an off-centre HI cloud (Oosterloo, Da Costa & Staveley-Smith 1996; Young & Lo 1997; St-Germain et al. 1999). The origin of this cloud is not clear, although it may be formed from supernovae winds associated with the most recent epoch of star formation in the galaxy (Young et al. 2007). Though there have been a number of optical studies of Phoenix, this seems to be the first to describe JHK_s observations.

2 OBSERVATIONS

Images centred on Phoenix were obtained over a period of about 3 years. A single observation comprises 10 dithered 30-s exposures which were reduced by means of the standard SIRIUS pipeline (Nakajima private communication). Normally, three such sets of frames were combined to give an effective 900-s exposure in each of J, H and K_s; when the seeing was poor, we combined six sets for an 1800-s exposure. Standard stars from Persson et al. (1998) were observed on each night and the results presented here are on the natural system of the SIRIUS camera, but with the zero-point of the Persson et al. standards. These magnitudes are expected to be close to those on the 2MASS system (Kato et al. 2007). The field of view is 7.8×7.8 arcmin, but this is reduced to 7.2×7.2 arcmin during the course of the reductions. The scale is 0.45 arcsec pixel^{-1}. According to Canterna & Flower

(1977) the optical size of Phoenix is 7×9 arcmin. Thus our observations cover most of the galaxy.

Table 1 contains our JHK_s results for all single stars measured on the images of Phoenix obtained for this investigation, together with positions allowing cross-identifications to the optical photometry of Massey et al. (2007; henceforth M2007), our identification number (N) which will be used in the text, and, in the last column, the I magnitude derived from M2007. Mean JHK_s magnitudes from all frames in each colour were used in compiling the table. The limiting magnitude is about 17.65 in K_s where the typical internal error is 0.04 mag; typical errors in J and H are 0.03 mag or less. Table 3 contains individual observations and dates of the two red variables found in our work, which are discussed in section 4.

The K_s and J frames were compared visually to check for possible very red AGB stars, but none was found redder than the Mira (see section 4), down to $K_s \sim 17$ mag.

3 COLOUR-MAGNITUDE AND COLOUR-COLOUR DIAGRAMS

Fig. 1 shows the $K_s, (J - K_s)$ diagram and Fig. 2 the $(J - H), (H - K_s)$ diagram for all single stars measured on the images centred on Phoenix that were obtained for this investigation. The photometry reduction program considered another five objects as double, and these were not plotted as the individual magnitudes were too uncertain. In discussing these figures we assume a distance modulus of 23.1 mag for Phoenix (see section 4). The blue stars in a vertical sequence with $(J - K_s) \sim 0.4$ in Fig. 1 are almost certainly field stars. This can be seen, for instance, by comparing with the similar figures in Menzies et al. (2002; henceforth JWM2002) for Leo I, obtained with the same instrumental arrangement. There are somewhat fewer of these stars in the Phoenix field. This is probably due to the higher galactic latitude ($b = -69$ (Phoenix); $b = +49$ (Leo I)). Other stars which are likely to be field stars (see below) are also marked as asterisk-shaped symbols. In Fig 2. the clear separation of many of the likely field stars from the members is apparent. There is some similarity of the distribution of points in this diagram with that for Leo I (JWM2002); there is a clump of stars with $(H - K_s) < 0.3$ as in Leo I, and a few redder ones that in Leo I are all carbon stars and mostly variable. A comparison between Phoenix and Leo I is made below (see section 3). The two carbon stars discovered by Da Costa (1994) are also marked on these figures.

The interpretation of the colour-magnitude diagram and the elimination of likely foreground stars is helped considerably by combining our data with the optical photometry of Massey et al. (2007). This is particularly important in establishing the AGB population of the galaxy. Held et al. (1999) have suggested (see their fig. 11) that there is a significant population of AGB stars in Phoenix with $I < 19.5$ and $(B - I) > 3.0$, but the separation from field stars is difficult (cf. Martinez-Delgado et al. 1999).

Fig 3(a) is a $(V - R), (B - V)$ diagram for objects with $I < 19.5$ and quoted uncertainties in both co-ordinates less than 0.1 mag from the observations of M2007. These cover an area of 34 x 34 arcmin centred on Phoenix. Since this area is much larger than the galaxy itself, the bulk of the stars

Table 1. Positions and IR photometry for all single stars measured on the images of Phoenix obtained for this investigation.

RA (J2000.0)	Dec	N	K_s	J-H	H-Ks	J-Ks	I
27.70577	-44.47683	50	16.93	0.65	0.04	0.68	18.34
27.70883	-44.43503	122	17.54	0.71	0.08	0.78	19.16
27.71133	-44.42600	129	17.46	0.69	0.07	0.76	19.11
27.71861	-44.50923	8	15.36	0.71	0.17	0.88	17.24
27.72032	-44.48024	49	16.69	0.36	-0.07	0.29	17.37
27.72356	-44.46934	88	17.11	0.76	0.11	0.87	18.98
27.72534	-44.49939	26	15.79	0.36	0.02	0.39	–
27.73110	-44.44578	107	17.36	0.82	0.06	0.88	19.21
27.73291	-44.41672	13	15.19	0.64	0.07	0.70	16.69
27.73303	-44.42099	131	17.55	0.75	0.04	0.80	19.26
27.73541	-44.43295	123	17.39	0.81	0.13	0.94	19.26
27.73560	-44.48583	81	17.03	0.59	0.18	0.77	19.26
27.73603	-44.47464	31	15.69	0.65	0.17	0.82	17.73
27.73785	-44.43591	121	17.28	0.57	0.22	0.79	–
27.74408	-44.41630	134	17.31	0.78	0.16	0.93	19.17
27.74641	-44.44115	3	13.15	0.64	0.04	0.69	–
27.74851	-44.48817	46	16.52	0.88	0.11	0.98	18.64
27.75006	-44.44932	2	13.11	0.50	0.01	0.51	80.00
27.75215	-44.42229	130	17.12	0.75	0.09	0.84	18.88
27.75259	-44.46943	52	16.59	0.85	0.09	0.94	18.61
27.75265	-44.44532	108	17.46	0.66	0.03	0.69	18.89
27.75280	-44.44059	120	17.44	0.81	0.12	0.93	19.52
27.75411	-44.47115	51	15.03	1.19	0.89	2.08	–
27.75417	-44.44467	112	17.32	0.66	0.03	0.70	18.78
27.75427	-44.45249	12	15.39	0.83	0.12	0.95	17.42
27.75427	-44.45694	7	14.49	0.44	-0.01	0.43	–
27.75441	-44.44759	32	15.88	0.72	0.09	0.81	17.54
27.75442	-44.44666	105	17.68	0.42	0.01	0.42	18.23
27.75659	-44.40777	136	17.56	0.67	0.05	0.71	19.16
27.75774	-44.45494	97	17.33	0.83	0.11	0.94	19.25
27.75827	-44.44532	56	16.54	0.86	0.13	0.99	18.64
27.76108	-44.41770	133	17.34	0.75	0.10	0.85	19.18
27.76173	-44.44854	55	16.49	0.75	0.07	0.82	18.18
27.76268	-44.44494	110	17.47	0.82	0.07	0.89	19.23
27.76659	-44.48769	47	16.58	0.67	0.10	0.77	18.22
27.76702	-44.44343	114	17.65	0.59	0.07	0.66	19.00
27.76729	-44.45500	96	17.44	0.75	0.10	0.84	19.24
27.76815	-44.45673	94	17.60	0.80	0.12	0.92	19.40
27.76831	-44.48687	48	16.64	0.62	0.17	0.79	18.38
27.76916	-44.42640	5	13.95	0.38	-0.00	0.38	–
27.76964	-44.45859	6	14.32	0.59	0.17	0.76	16.11
27.77019	-44.48075	83	17.20	0.74	0.10	0.84	19.00
27.77352	-44.48684	80	17.30	0.82	0.13	0.94	19.13
27.77360	-44.43816	33	15.94	0.87	0.27	1.14	18.24
27.77402	-44.49752	10	15.47	0.36	-0.00	0.36	16.24
27.77405	-44.45512	53	16.24	0.68	0.14	0.82	18.05
27.77557	-44.43107	125	17.56	0.81	0.12	0.93	19.43
27.77731	-44.44379	113	17.46	0.75	0.10	0.85	19.23
27.77740	-44.43351	60	16.73	0.82	0.14	0.96	18.69
27.77798	-44.45670	93	17.43	0.80	0.13	0.93	19.36
27.77821	-44.50607	71	17.22	0.78	0.15	0.92	19.08
27.77984	-44.44510	109	17.48	0.82	0.10	0.91	19.36
27.78000	-44.45448	98	17.38	0.83	0.13	0.96	19.29
27.78031	-44.44961	104	17.05	0.74	0.08	0.83	18.82
27.78081	-44.44227	116	16.83	0.87	0.36	1.23	–
27.78131	-44.45070	103	17.50	0.74	0.14	0.88	19.25
27.78158	-44.48930	78	17.09	0.67	0.11	0.78	18.60
27.78170	-44.45373	99	17.62	0.84	0.10	0.94	19.51
27.78273	-44.41102	14	14.72	0.41	0.03	0.44	15.25
27.78391	-44.45143	101	17.29	0.83	0.09	0.92	19.20
27.78412	-44.47465	86	17.46	0.77	0.09	0.86	19.26
27.78465	-44.47567	84	17.53	0.76	0.12	0.88	19.39

Table 1. Continued

RA (J2000.0)	Dec	N	K_s	J-H	H-Ks	J-Ks	I
27.78534	-44.50643	41	16.59	0.82	0.17	1.00	18.68
27.78607	-44.45109	54	16.80	0.68	0.08	0.76	18.35
27.78643	-44.42723	128	17.48	0.69	0.23	0.91	19.48
27.78651	-44.43156	124	17.29	0.81	0.11	0.93	19.23
27.78669	-44.44216	117	17.75	0.72	-0.00	0.72	19.33
27.78671	-44.42488	34	15.25	1.05	0.53	1.57	19.48
27.78732	-44.47034	87	16.90	0.81	0.15	0.96	19.00
27.78837	-44.48860	4	13.30	0.45	0.01	0.46	–
27.79029	-44.47513	85	17.37	0.83	0.13	0.96	19.29
27.79328	-44.42856	126	17.02	0.79	0.12	0.91	19.00
27.79454	-44.51225	40	16.26	0.69	0.17	0.86	17.92
27.79501	-44.41957	61	16.76	0.65	0.06	0.71	18.29
27.79895	-44.45101	102	16.85	0.67	0.14	0.81	18.55
27.80202	-44.45618	95	17.54	0.77	0.10	0.87	19.32
27.80302	-44.40294	35	16.01	0.58	0.09	0.67	17.49
27.80355	-44.40904	135	17.53	0.76	0.13	0.89	19.41
27.80573	-44.46179	91	17.43	0.78	0.02	0.81	19.13
27.80617	-44.50018	72	17.55	0.67	0.07	0.74	19.67
27.80866	-44.46093	92	17.57	0.83	0.11	0.93	19.43
27.80904	-44.44226	57	16.56	0.87	0.16	1.04	18.78
27.81347	-44.50706	70	17.43	0.78	0.14	0.91	19.27
27.81846	-44.40759	137	17.36	0.74	0.04	0.79	19.19
27.81927	-44.51210	69	17.33	0.67	0.17	0.83	18.95
27.82514	-44.39088	62	16.63	0.56	0.23	0.79	–
27.82563	-44.45501	11	15.37	0.68	0.12	0.81	17.15
27.82798	-44.46254	90	17.55	0.78	0.08	0.85	19.33
27.83021	-44.44322	115	17.63	0.71	0.05	0.76	19.28
27.83413	-44.39202	141	17.55	0.59	0.25	0.84	19.45
27.83445	-44.48040	30	15.66	0.71	0.07	0.78	17.28
27.83794	-44.44127	118	17.53	0.79	0.14	0.93	19.38
27.83868	-44.46736	89	17.25	0.61	0.18	0.79	18.97
27.84202	-44.45187	100	17.59	0.40	0.12	0.52	18.15
27.84331	-44.42792	127	17.60	0.77	0.19	0.95	19.48

Table 2. Stars in common with Da Costa (1994).

DaCosta	vdRDK	This	Spectroscopy
C1	481	87	carbon
C2		52	not carbon
C3	391?	88	not carbon
C4	166	102	carbon
C5		106	not carbon

Note: Stars originally selected by M Irwin. vdRDK: van de Rydt et al. (1991),

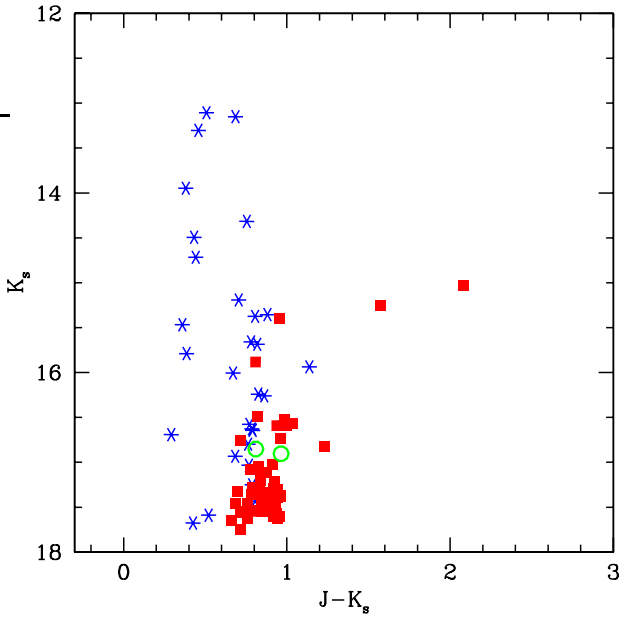

Figure 1. Colour-magnitude diagram for the field centred on Phoenix. Asterisk symbols are probable field stars (i.e. they lie above the dashed line in Fig 3(a)). Filled squares are probable members, while the two known carbon stars are shown as open circles.

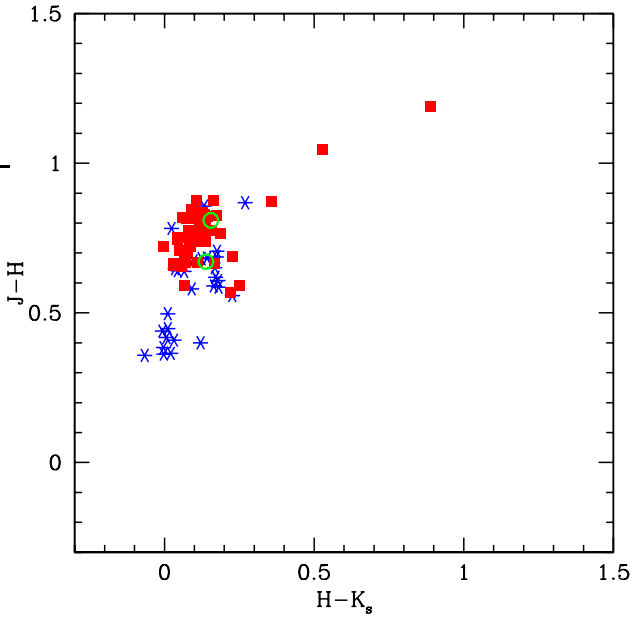

Figure 2. $(J-H),(H-K_s)$ two-colour diagram for the Phoenix field. Symbols as for Fig. 1.

plotted are field objects. In particular, the heavily populated areas in this diagram are likely to contain a high proportion of field stars. Especially at the redder colours the stars in this diagram divide rather clearly into two groups (presumably giants and dwarfs). The dashed line, extrapolated to bluer colours, approximately marks this division.

In Fig 3(b) the dashed line from Fig 3(a) is repeated and stars in common between out survey and M2007 are plotted. The curves show the loci of normal giants and dwarfs. Using the division into two sequences and the density of the M2007 points in Fig 3(a), we divide our stars into probable field stars (asterisks) and probable Phoenix members (squares). The differing distribution of the stars in the whole M2007 sample and those in common with our survey, strongly suggests that the stars below the dashed line (the likely giant region) have a high probability of being Phoenix members and we have taken them as such. Note particularly the concentration of stars in common, below the dotted line and with $\sim 1.4 < (B-V) <\sim 1.55$, strongly indicating membership. The Bahcall-Soneira model (Bahcall & Soneira 1980)

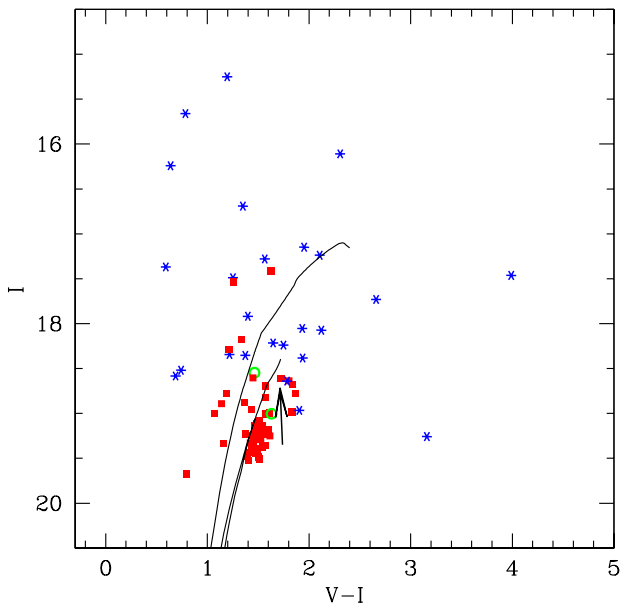

Figure 4. $I,(V-I)$ colour-magnitude diagram for stars in Phoenix measured in this programme. Symbols as in Fig. 1. The curves illustrate isochrones from Girardi et al. (2000, 2002) for two populations, one with age 14 Gyr and metallicity z=0.001 and the other with age 1 Gyr and z=0.002. The two red variables, with $(J-K_s) > 1.4$, do not have $I,(V-I)$ photometry and thus cannot be included in the figure. Star C2 (our number 52) is marked with an arrow.

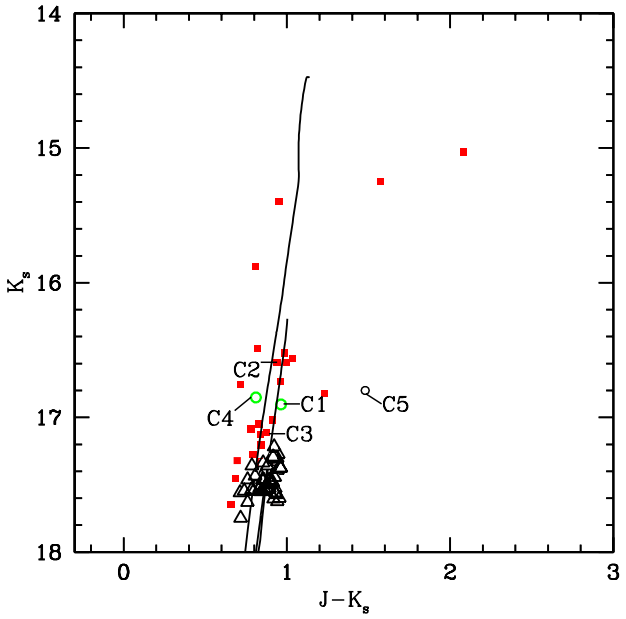

Figure 5. $K_s,(J-K_s)$ colour-magnitude diagram for Phoenix showing only the probable members. Open triangles indicate stars with $I > 19.05$, corresponding to the majority old population RGB in Phoenix. Other symbols are as in Fig. 1 and isochrones are as in Fig. 4.

predicts 24 field stars with $V < 20$ for a field of our size at $b = 90$ and 32 at $b = 50$, $l = 270$ (Phoenix has $b = -69$, $l = 272$). In view of the small number statistics the number of stars rejected here (35) seems to be of the correct order. Fig. 4 is an $I, V-I$ diagram of stars in common with M2007 with field stars and members distinguished. The distribution of probable field stars in this figure supports their classification as such.

There is a sparse population of young, blue, stars in Phoenix. This has an upper brightness limit of about $V = 19$ (M2007 fig. 20). Since the $V-K_s$ colours of these stars must be within a few tenths of a magnitude of zero, they will be too faint to be in our survey.

Figs. 5 and 6 are $K_s,(J-K_s)$ and $(J-H),(H-K_s)$ plots for Phoenix with the likely field stars removed. In Figs. 4 and 5 we show isochrones (RGB and AGB) for z = 0.001, age 14 Gyr and z = 0.002, age 1 Gyr from Girardi et al. (2000, 2002). The RGB tip (TRGB) for the 14 Gyr model occurs at $K = 17.17$ and $I = 19.06$ (i.e. very close to the values observed, as will be discussed below), while that for the 1 Gyr model is at $K = 19.87$ and $I = 21.17$[1]. Note that the isochrones provide only a qualitative illustration of the populations which might be present and they suggest that the members of the dwarf galaxy are on the RGB and AGB of a population with a large range of ages. These late stages of stellar evolution are not well understood and

[1] As will be discussed in section 4, the reddening of the Phoenix stars is small enough to be neglected in these comparisons with isocrones.

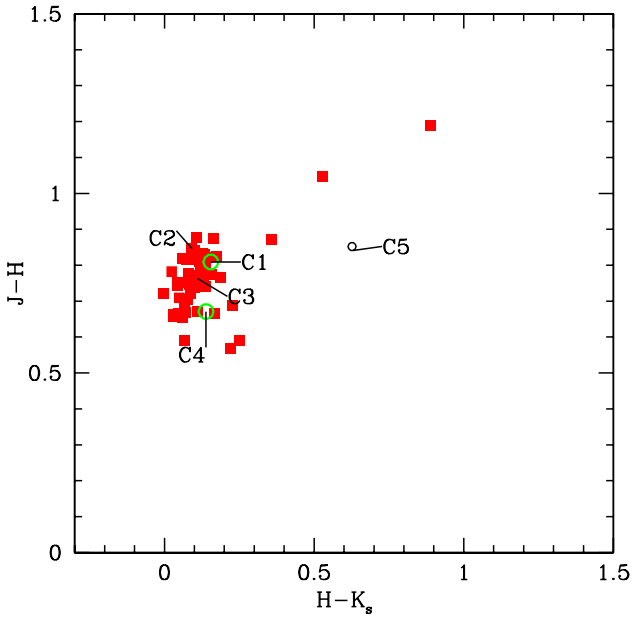

Figure 6. $(J-H),(H-K_s)$ two-colour diagram for Phoenix, without the probable field stars. Symbols as in Fig. 1.

models by different authors provide significantly different tracks, e.g. AGB isochrones from Pietrinferni et al. (2004) terminate several magnitudes fainter than those illustrated. Furthermore, there are as yet no examples of AGB models which provide a good fit to observations over a range of wavelengths.

M2007 suggest that Phoenix may contain a population

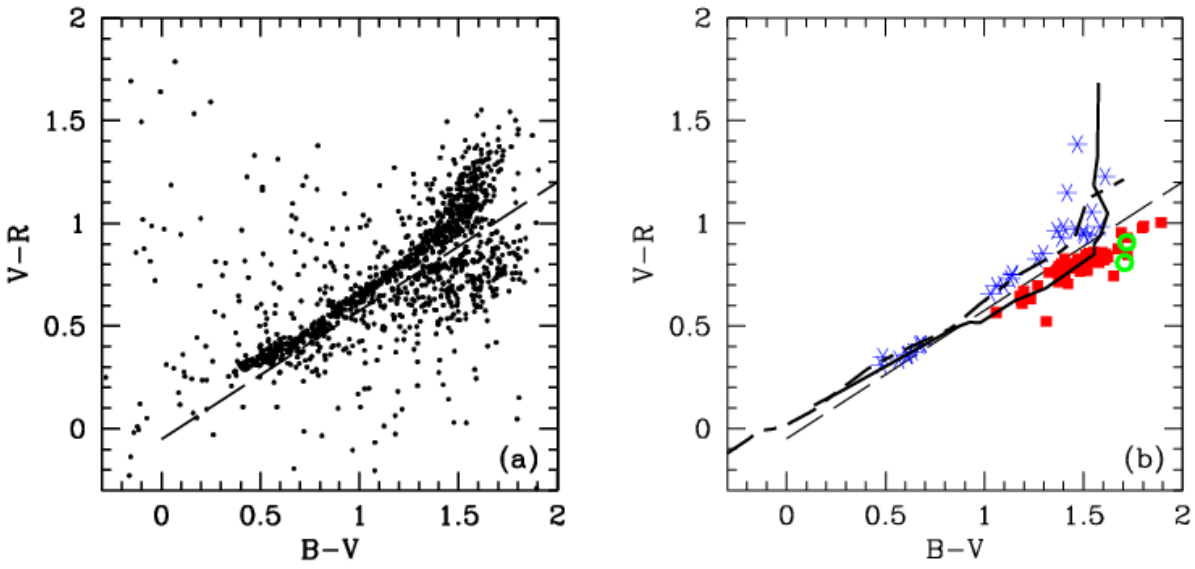

Figure 3. (a)$(V-R),(B-V)$ two-colour diagram for the Phoenix field. Small squares represent stars from M2007 (see text). The long-dashed line shows our proposed separation between field and Phoenix stars. (b)Stars in our survey in common with M2007 are plotted in a $(V-R),(B-V)$ two-colour diagram, with asterisk symbols being probable field stars and filled squares probable Phoenix members; the two carbon stars are indicated by open circles. Dash-dot and continuous lines represent standard dwarf and giant sequences (derived from Bessell (1990)).

of yellow supergiants, though they recognize that it is difficult in their work to distinguish galaxy members from foreground stars. Since their yellow supergiant sequence extends up to V of about 15 mag and since $V-K_s$ may well be significant (1 or greater), it seems possible that the bright star in Fig. 5 with $J-K_s$ of about 0.9 and K_s of about 15.3 may be such a star.

The absolute magnitude of the TRGB in K_s depends on metallicity and age. Estimates of the metallicity of the old population of Phoenix ranging from –1.37 to –1.8 have been given (Gallart et al. 2004; Holtzman et al. 2000; Held et al. 1999). If the main population of Phoenix is of globular cluster age and has a metallicity of ~ -1.3 we would expect the TRGB to be at $M_K \sim -5.8$ (Salaris & Girardi 2005), corresponding to $K_s = 17.3$ in Phoenix. We would then identify the near vertical, sequence of stars with $(J-K_s) \sim 0.9$ and fainter than $K_s \sim 17.1$ as mainly due to this population. Such a population will not produce normal, intrinsic, carbon stars, which are expected to belong to an intermediate age population. The possibility that these objects are extrinsic carbon stars seems remote, especially since they lie above the TRGB of even the old population (see section 4).

Our identification of the TRGB of the main population at $K_s \sim 17.1$ is entirely consistent with data at other wavelengths. The presence of a TRGB in the range $I = 19.25$ to 19.00 was clearly established in the work of van de Rydt et al. (1991), Martinez-Delgado et al. (1999), Held et al. (1999), and Holtzman et al. (2000). Table A1 of our appendix shows that all our probable AGB stars have I magnitudes brighter than this. (The only one close to the tip is one of the carbon stars). A TRGB near $I = 19.0$ is also evident in Fig. 4 and the stars there are those showing a tip at $K_s \sim 17.0$ in Fig. 5. One can also compare the results for Phoenix with RGB predictions. The recent review by Bellazzini (2007), his fig. 5, leads to a predicted TRGB at $K \sim 16.94$ for a colour at the tip of $(J-K) \sim 0.9$ as in our case and for our adopted distance modulus. As regards I, his fig. 4 (or his eq. 2, corrected for errors in sign) leads to a TRGB of ~ 19.08 at our adopted distance and with $(V-I)_o = 1.48$ at the tip (Held et al. 1999). Evidently there is good consistency between the results from the TRGB at I and that at K_s.

In addition to finding two carbon stars, Da Costa (1994) obtained spectra of three other stars in which he found no evidence of carbon-star features; we presume these to be oxygen-rich. They are listed in Table 3 with their identifications from van de Rydt et al. (1991) and our numbers. The non-carbon stars are also marked in Figs. 5 and 6. C5 is a double, possibly of field dwarfs. C2 and C3 are among our presumed members. The position of C3 in Fig. 5, immediately below the two C stars, suggests that it may be an intermediate age star marking a lower limit to carbon star formation or it may be a member of the old population and near its TRGB.

In Fig. 5 there are a number of stars fainter than $K_s \sim 17.2$ which are plotted as squares because they have I magnitudes brighter than the TRGB (they are mainly in the range $I \sim 18.5$ to 19.0. In both Figs. 4 and 5 these stars lie to the blue of the main concentrations. The most likely explanation of these stars is that they are AGB stars of an intermediate age population and may well be coeval with the carbon stars.

The seven stars immediately above the two carbon stars (and slightly redder) in Fig. 5 constitute an interesting problem. Table A1 in the appendix lists optical and infrared data for these stars and for the two spectroscopic carbon stars.

Evidently the seven stars have colours rather similar to the known carbon stars and on these grounds would be strong C star candidates. This, together with their position immediately above the C stars in Fig. 6, would be entirely in accord with expectation (see for instance the distribution of C stars in the Leo I $K_s, (J-K_s)$ diagram (JWM2002). However, one of these stars, Da Costa C2, our No. 52, is not a spectroscopic carbon star. The nature of this star and possibly of the other six stars in this group remains to be determined.

Table A2 in the appendix lists standard infrared sequences for giants and dwarfs from Bessell & Brett (1988) that have been converted to the 2MASS system (which is close to the IRSF system) using the relations in Carpenter (2001). Table A3 contains optical data for extreme subdwarfs listed by Gizis (1997) together with 2MASS data for these stars. Comparison of these tables with the data for our seven stars shows the following: their $J-H$ and $J-K_s$ are too red for them to be normal dwarfs. From their optical colours some, or all, of them (including C2 = 52) could be extreme subdwarfs (compare their positions in a plot such as fig. 9 of Gizis). However, their infrared colours are too red for such an assignment, being reasonably similar to those of late type giants. On the other hand, several have suspiciously red $B-V$ values both for normal giants and for metal-poor (globular cluster type) giants. Furthermore, as late-type giants they would be very distant (extragalactic) and thus strong Phoenix candidates. Comparison with the isochrones shown in Figs. 4 and 5 suggests that C2 is best interpreted as an AGB star of the very old population. Evidently, spectral type and radial velocity data are required for the other stars in this group to determine whether or not they are similar to C2 or whether they are carbon stars.

A comparison of Figs. 5 and 6 with the $K_s, (J-K_s)$ and $(J-H), (H-K_s)$ diagrams of the dwarf spheroidal Leo I (JWM2002) is of interest. The reddening of both galaxies is small and the distance modulus of Phoenix is ~ 1.0 mag greater than that of Leo I. The faintest known carbon stars in Leo I are at $K_s \sim 15.5$ and are thus intrinsically brighter by ~ 0.4 mag than the Da Costa (1994) carbon stars in Phoenix. The two very red and variable stars in Phoenix (see section 4) have $K_s \sim 15.2$ whilst there are red variables in Leo I with K_s in the range 13.8-14.5 and so roughly equivalent. However, there is a marked difference in the AGB between the two galaxies. In Leo I there is a well populated sequence of carbon stars extending from about $K_s, (J-K_s)$, 15.5, 0.9 to 13.9, 1.7. In Phoenix, whilst the low-amplitude variable (star 34) lies near the upper end of such a sequence at $K_s \sim 15.25$ and $(J-K_s) \sim 1.6$ there are no stars in this sequence between it and the small clump of stars containing C2. The difference between Phoenix and Leo I is even more marked, if, as discussed above the stars in this clump are not C stars. These differences are most likely related to the different star formation histories of these dwarf galaxies.

4 VARIABLE STARS AND DISTANCE

As Figs. 1 and 2 show there are two outstanding red stars in Phoenix. We find both stars to be variable. The JHK_s observations are listed in Table 3 with the Julian Dates for the observations. Star number 34 is a low amplitude variable. No convincing period is evident in our measures though it varies on a time scale of 200 to 300 days. The JHK_s measurements for this star in Table 1 are simply the means of the individual values in Table 3.

Table 3. JHK_s photometry for two red variables in Phoenix.

JD	J	σ_J	H	σ_H	K_s	σ_K
			Star 51			
2507.11817	17.979	0.024	16.610	0.014	15.562	0.013
2813.14560	16.961	0.008	15.717	0.004	14.860	0.005
2881.02012	17.652	0.014	16.237	0.007	15.190	0.005
2962.85237	18.070	0.030	16.655	0.009	15.498	0.008
3010.80022	18.051	0.039	16.618	0.010	15.410	0.008
3173.12370	16.577	0.009	15.479	0.008	14.718	0.009
3256.06266	16.981	0.010	15.763	0.010	14.848	0.010
3260.06350	16.993	0.009	15.798	0.009	14.879	0.005
3292.92197	17.271	0.014	16.020	0.010	15.059	0.010
3349.86790	17.565	0.020	16.315	0.009	15.242	0.011
3352.82444	17.579	0.017	16.308	0.009	15.302	0.009
3440.73494	17.204	0.026	16.044	0.016	15.143	0.014
3531.16565	16.284	0.009	15.351	0.007	14.711	0.008
3612.08834	16.372	0.015	15.308	0.010	14.692	0.020
3615.01896	16.412	0.010	15.361	0.009	14.684	0.009
			Star 34			
2507.11817	16.881	0.010	15.819	0.008	15.286	0.011
2813.14560	17.033	0.012	15.942	0.004	15.345	0.005
2881.02012	16.887	0.010	15.846	0.005	15.265	0.006
2962.85237	16.823	0.010	15.807	0.007	15.259	0.009
3010.80022	16.805	0.014	15.749	0.007	15.221	0.008
3173.12370	16.916	0.012	15.839	0.009	15.272	0.009
3256.06266	16.833	0.010	15.777	0.008	15.269	0.009
3260.06350	16.822	0.009	15.782	0.010	15.255	0.007
3292.92197	16.720	0.009	15.698	0.009	15.173	0.009
3349.86790	16.757	0.009	15.738	0.008	15.205	0.013
3352.82444	16.800	0.010	15.721	0.007	15.202	0.009
3440.73494	16.889	0.019	15.816	0.014	15.287	0.015
3531.16565	16.617	0.013	15.653	0.010	15.162	0.010
3612.08834	16.814	0.020	15.769	0.015	15.214	0.026
3615.01896	16.699	0.009	15.673	0.009	15.199	0.009

Star 51 is a large amplitude (Mira) variable with P = 425 ± 25 days, Fourier mean magnitudes of $J = 17.11, H = 15.92, K_s = 15.03$ and $\Delta K_s = 0.76, \Delta J = 1.52$. Light curves are shown in Fig. 7. The J light curve clearly shows that the star was brightening on a long time scale during the time of our observations. This is typical behaviour for a carbon Mira (e.g. Whitelock et al. 2006). Such stars are obscured from time to time owing to the ejection of material into the line of sight.

Previous authors (van de Rydt et al. 1991, Martinez-Delgado et al. 1999, Held et al. 1999, Holtzman et al. 2000) have adopted a reddening of $E(B-V) = 0.02$ mag from the work of Burstein & Heiles (1982) and we adopt this value. Whilst there is undoubtedly some uncertainty in this, the reddening at the galactic latitude of Phoenix ($b = -69$) must be small and any reasonable change will have little or no effect on our discussion. Then, converting the photometry to the SAAO system using the relations of Carpenter (2001) we obtain for the Mira (star 51) $K_0 = 15.01, (H-K)_0 = 0.90, (J-K)_0 = 2.20$ and $m_{bol} = 18.51$. Here the bolometric correction to K was derived from the relation given by Whitelock et al. (2006, their equation 10), which is derived for carbon stars. We assume both this star and the other

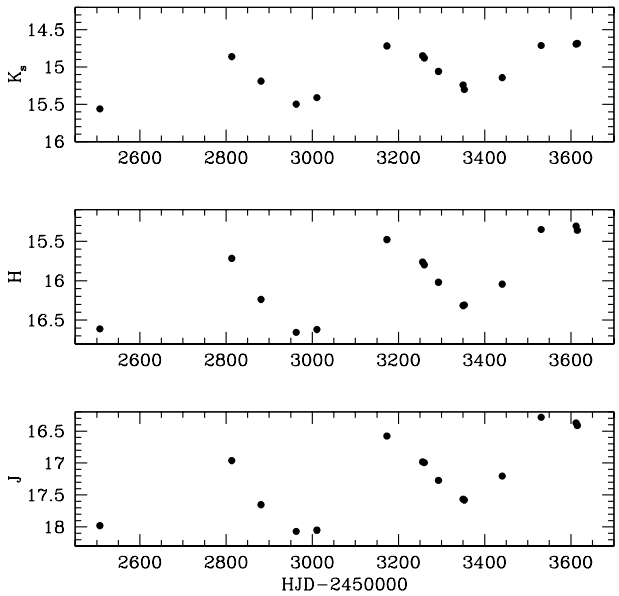

Figure 7. The JHK_s light curves of the Mira variable (star 51 in Table 1).

variable are carbon stars in view of their red colours and the presence of other carbon stars in the galaxy.

The Mira (star 51) is the candidate long period variable ID 11263 of Gallart et al. (2004). For this star their mean results are $I = 18.90, (B-V) = 4.38, V-I = 2.29$. It is the reddest likely member in their $I-(V-I)$ diagram. Since it lies on a reasonable extension of the RGB/AGB and not fainter as it would be if it suffered from strong circumstellar extinction, the very red $(B-V)$ must be mainly intrinsic to the star and is consistent with its being a carbon star rather than a highly reddened oxygen-rich Mira. Comparison with figs. 7 and 8 of Whitelock et al. (2006) shows that in $(J-H), (H-K_s)$ diagrams the two Phoenix variables lie close to Galactic and LMC carbon-rich Miras and SR variables. In an $(H-K_s), \log P$ diagram (Whitelock et al. 2006, fig. 11) the Phoenix Mira lies in the region occupied by Galactic carbon Miras and bluer than the known LMC carbon Miras, except for two LMC stars believed to be undergoing hot-bottom burning (HBB). It is unlikely that it is an HBB star (see below). Whether this difference from the LMC carbon stars is significant or not depends at least partly on whether Phoenix contains redder (i.e. more dust enshrouded) stars which might be below our detectable brightness limit.

Of the six candidate LPVs identified by Gallart et al. (2004) only three fall in the area we surveyed. One of these is the Mira discussed above the other two are our numbers 88 (their ID 11200) and 102 (their ID 8563). The photometry of these two stars has marginally larger standard deviations in all colours than stars of corresponding brightness, but there is no clear periodicity in either. Note that star 102 is a Carbon star (C4 of Da Costa) and the star 88 is NOT a Carbon star (C3 of Da Costa). No other stars brighter than $K_s = 17.4$ show any convincing evidence of variability with amplitude greater than 0.1mag.

An estimate of the distance modulus of Phoenix can be made using absolute magnitudes in either K or M_{bol} derived from period luminosity relations. In the case of K we use the relation:

$$M_K = -3.30 \log P + 0.59. \quad (1)$$

The slope of this relation was derived from carbon Miras in the LMC by Feast et al. (1989), and we have assumed an LMC distance modulus of 18.39 ± 0.05 (van Leeuwen et al. 2007). For M_{bol} we adopt

$$M_{bol} = -2.54 \log P + 1.98, \quad (2)$$

again from LMC carbon Miras but now including some heavily dust-enshrouded members (Whitelock et al. 2006) and the same distance modulus. It should be noted that a Galactic zero-point for this relation (2.06 ± 0.24 (Feast et al. 2006)) is close to the value used.

With these absolute magnitudes we derive distance moduli of 23.09 ± 0.19 from M_K and 23.10 ± 0.18 from M_{bol} where the uncertainties take into account both the scatter about the PL relations and the uncertainty in the distance modulus of the LMC. Held et al. (1999) quote moduli of 23.21 ± 0.08 from the horizontal branch (HB) at V and 23.04 ± 0.07 from the TRGB at I. Martinez-Delgado (1999) also used the latter method to obtain a modulus of 23.0 ± 0.1. Holtzman et al. (2000) obtained 23.1 from the TRGB and 23.3 from an assumed absolute magnitude of the HB. These estimates all agree well and we adopt 23.1 for the galaxy.

M2007 find a reddening of $E(B-V) = 0.15$ from a study of the young population of Phoenix. Adopting such a reddening would decrease the modulus derived from the Mira by only about 0.04 mag. But the Held et al. (1999) values would be considerably affected; the moduli from the HB and from the TRGB would both become 22.81. However, the M2007 reddening is likely to apply only to the small young population in Phoenix. Note that if the Phoenix Mira were an HBB star (as discussed above) it would be expected to be brighter than the PL relations used here suggest. So the agreement with other distance moduli noted in the previous paragraph is an indication that it is not an HBB star.

5 CONCLUSIONS

By combining our own JHK_s observations with the optical photometry of Massey et al. (2007) it has been possible to make a rather clean separation of Phoenix members from field stars. A clear RGB of an old population is found together with a few highly evolved stars. A Mira variable, almost certainly a carbon star, with a period of 425 days is present in the galaxy and leads to an estimate of 23.10 ± 0.18 for the distance modulus in agreement with other estimates. The kinematics of carbon Miras in our Galaxy (Feast et al. 2006) suggest an age of ~ 2 Gyr for this star. Since Miras are relatively short-lived objects this implies a significant population of this age.

The two Da Costa carbon stars have $M_K = -6.2$ or $M_{bol} = -3.8$ (based on an estimate of the bolometric correction from the work of Frogel et al.(1980)). These luminosities are consistent with an age ~ 1 to a few Gyr (see e.g. the luminosities of carbon stars in LMC clusters (Frogel et al. 1990)). Whilst most of the stars fainter than $K_s \sim 17.2$

are found to be members of an old RGB population, a significant number of them are identified as probably AGB stars of intermediate age. They are likely to belong to the same population as the carbon stars. In this connection, we note that a feature in the colour-magnitude diagram of Holtzman et al. (2000) (their fig. 2), starting at V or I of ~ 24.0, $(V-I) \sim 0$ and sloping to higher luminosities and redder colours may be a subgiant branch of intermediate age stars. It is reasonably well fitted by a 1 Gyr isochrone (z = 0.002) from Girardi et al. (2002).

The status of the non-carbon star Da Costa C2 which is ~ 0.3 mag brighter than the two carbon stars at K_s is uncertain. It seems most likely to be an AGB star of an old population. Whether other stars of about the same luminosity and colour to C2 are also old AGB stars or carbon stars of an intermediate age population requires further spectroscopic work.

ACKNOWLEDGMENTS

We are grateful to the IRSF/SIRIUS team, based in Nagoya University, Kyoto University the National Astronomical Observatory of Japan, for their support during our observations. We also acknowledge our Japanese colleagues, T. Tanabé, Y. Ita, S. Nishiyama, R. Kadowaki, A. Ishihara, Y. Haba and J. Hashimoto, for obtaining for us some of the images of Phoenix that were used in this investigation. Dr P. Massey very kindly sent us the Phoenix observations obtained by himself and his colleagues in advance of publication.

REFERENCES

Aaronson M., Blanco V. M., Cook K. H., Schechter P. L., 1989, ApJS, 70, 637
Bahcall J. N., Soneira R. M., 1980, ApJS, 44, 73
Bellazzini M., 2007, arXiv:0711.2016
Bessell M. S., 1990, PASP, 102, 1181
Bessell M. S., Brett J. M., 1988, PASP, 100, 1134
Burstein D., Heiles C., 1982, AJ, 87, 1165
Canterna R., Flower, P. J., 1977, ApJ, 212, 57L
Carpenter J. M., 2001, AJ, 121, 2851
Da Costa G. S. 1994, in: ESO Conf. Workshop Proc. 49, Dwarf Galaxies: Proc. ESO/OHP Workshop, eds. G. Meylan & P. Prugniel (Garching: ESO), 221
Feast M. W., Whitelock P. A., Menzies J.W., 2006, MNRAS, 369, 791
Frogel J. A., Persson S. E., Cohen J. G., 1980, ApJ, 239, 495
Frogel J. A., Mould J., Blanco V. M., 1990, ApJ, 352, 96
Gallart C., Aparicio A., Freedman W. L., Madore B. F., Martínez-Delgado, D., Stetson P. B., 2004, AJ, 127, 1486
Girardi L., Bressan A., Bertelli G., Chiosi C., 2000, A&ASup, 141, 371
Girardi L., et al., 2002 http://stev.oapd.inaf.it/lgirardi/cgi-bin/cmd
Gizis J. E., 1997, AJ, 113, 806
Grebel E., 1999, in: (eds.) Whitelock P. & Cannon R., The stellar Content of Local group Galaxies, IAU Sym. 192, ASP, p. 17
Held E. V., Saviane I., Momany Y., 1999, A&A, 345, 747
Holtzman J. A., Smith G. H., Grillmair C., 2000, AJ, 120, 3060
Martinez-Delgado D., Gallart C., Aparicio A., 1999, AJ, 118, 862
Massey P., Olsen K. A. G., Hodge P. W., Jacoby G. H., McNeill R. T., Smith R. C., Strong S. B., 2007, AJ, 133, 2393 (M2007)
Mateo M., 1998, ARA&A, 36, 435
Menzies J., Feast M., Tanabé T., Whitelock P.A., Nakada Y., 2002, MNRAS, 335, 923 (JWM2002)
Nagashima C. et al., 1999, in Star Formation 1999, ed. T. Nakamoto (Nobeyama: Nobeyama Radio Observatory) 397
Nagayama T. et al., 2003, Proc. SPIE 4841, 459
Oosterloo T., Da Costa G. S., Staveley-Smith L., 1996, AJ, 112, 1969
Persson S. E., Murphy D. C., Krzeminski W., Roth M., Rieke M. J., 1998, AJ, 116, 2457
Pietrinferni A., Cassisi S., Salaris M., Castelli F., 2004, ApJ, 612, 168
Salaris M., Girardi L., 2005, MNRAS, 357, 669
Schuster H. E., West R. M., 1976, A&A, 49, 129
St-Germain J., Carignan C., Côte S., Oosterloo T., 1999, AJ, 118, 1235
van de Rydt F., Demers S., Kunkel W. E., 1991, AJ, 102, 130
Whitelock P. A., Feast M. W., Marang F., Groenewegen M. A. T., 2006, MNRAS, 369, 751
Young L. M., Lo, K. Y., 1997, ApJ, 490, 710
Young L. M., Skillman E. D., Weisz D. R., Dolphin A. E., 2007, ApJ, 659, 331

APPENDIX

Table A1. IRSF data for the non-variable assumed AGB stars more luminous than the C stars.

No.	K_s	$J-H$	$H-K_s$	$J-K_s$	V	$B-V$	$V-R$	$R-I$	$V-I$	$V-K_s$	I
52 (C2)	16.59	0.85	0.09	0.94	20.335	1.720	0.929	0.796	1.725	3.75	18.610
56	16.54	0.86	0.13	0.99	20.423	1.532	0.940	0.844	1.784	3.88	18.639
55	16.49	0.75	0.07	0.82	19.512	1.422	0.706	0.626	1.332	3.02	18.180
60	16.73	0.82	0.14	0.96	29.266	1.510	0.843	0.730	1.573	3.54	18.693
41	16.59	0.82	0.17	1.00	20.514	1.797	0.978	0.857	1.835	3.92	18.679
61	16.76	0.65	0.06	0.71	19.507	1.177	0.645	0.572	1.217	2.75	18.290
57	16.56	0.87	0.16	1.04	20.649	1.892	1.003	0.868	1.871	4.09	18.778
Carbon stars											
87	16.90	0.81	0.15	0.96	20.636	1.718	0.907	0.725	1.632	3.74	19.004
102	16.85	0.66	0.14	0.81	20.010	1.707	0.808	0.655	1.463	3.16	18.547

Table A2. 2MASS data for Bessell & Brett's (1988) dwarfs and giants.

Sp	$V-K_s$	$J-H$	$H-K_s$	$J-K_s$	$V-K_s$	$J-H$	$H-K_s$	$J-K_s$
	Dwarfs				Giants			
K0					2.35	0.48	0.12	0.60
K1					2.54	0.52	0.13	0.65
K2					2.74	0.57	0.14	0.71
K3					3.04	0.62	0.17	0.79
K4	2.67	0.52	0.13	0.65	3.30	0.67	0.18	0.85
K5	2.89	0.55	0.14	0.69	3.64	0.73	0.19	0.92
K7	3.20	0.60	0.16	0.76				
M0	3.69	0.64	0.19	0.83	3.89	0.77	0.22	0.99
M1	3.91	0.62	0.23	0.85	4.09	0.79	0.23	1.02
M2	4.15	0.61	0.24	0.85	4.34	0.81	0.24	1.05
M3	4.60	0.56	0.28	0.84	4.68	0.84	0.26	1.10
M4	5.30	0.54	0.30	0.84	5.14	0.87	0.27	1.14
M5	6.16	0.56	0.35	0.91	6.00	0.89	0.31	1.20
M6	7.34	0.60	0.40	1.00	6.88	0.90	0.33	1.23
M7					7.84	0.90	0.34	1.24

Table A3. Extreme cool subdwarfs from Gizis (1997); infrared photometry from 2MASS.

LHS	K_s	$J-H$	$H-K_s$	$J-K_s$	V	$V-K_s$	$B-V$	$V-R$	$R-I$	$V-I$
104	10.412	0.525	0.154	0.679	13.78	3.37	1.34	0.81	0.91	1.72
161	10.995	0.516	0.203	0.719	14.75	3.75	1.55	1.01	0.96	1.98
169	10.819	0.474	0.193	0.667	14.13	3.31	1.45	0.91	0.76	1.72
182	10.519	0.428	0.150	0.578	13.42	2.90	1.57			
185	11.517	0.618	0.221	0.839	15.30	3.78	1.79	0.98	0.85	1.83
364	10.860	0.451	0.155	0.606	14.61	3.75	1.71	1.03	0.92	1.95
375	11.507	0.476	0.167	0.643	15.68	4.17	1.87	1.08	1.12	2.20
489	11.852	0.474	0.205	0.679	15.48	3.63	1.69	0.91	0.86	1.77
522	10.927	0.480	0.177	0.657	14.15	3.22	1.41	0.84	0.78	1.62
1970	13.875	0.581	0.124	0.705	17.76	3.88	1.68			2.09
3382	13.197	0.520	0.147	0.667	17.02	3.82	1.99	1.03	1.06	2.09